Synergy-Based, Data-Driven Generation of Object-Specific Grasps for Anthropomorphic Hands

Julia Starke, Christian Eichmann, Simon Ottenhaus and Tamim Asfour

Abstract— Building anthropomorphic robotic and prosthetic hands is a challenging task due to size and performance requirements. As of today it is impossible for such artificial hands to mimic the capabilities of a human hand. A popular approach to reduce the complexity in hand design is the realization of hand synergies through underactuated mechanism, leading also to a reduction of control complexity. In this paper we aim to find grasp synergies of human grasps by employing a deep autoencoder. We perform a grasp study with 15 subjects including 2250 grasps on 35 diverse objects. The emerging latent space contains a comprehensive representation of grasp type and the size of the grasped object, while preserving a large amount of grasp information. In addition we report on novel findings on couplings and grasp specific features of joint kinematics, which can be directly applied to the control of anthropomorphic hands.

I. INTRODUCTION

The human hand is a highly complex system with 23 *Degrees of Freedom* (DOF) to perform versatile and dexterous grasping and manipulation tasks. It includes 34 muscles and more than three times as many tendons to conduct the broad set of motions we perform every day. With the development of anthropomorphic, five-fingered artificial hands, roboticists strive to transfer as much versatility as possible into robotic and prosthetic applications. However the complexity of the human hand issues vast challenges for the development of control strategies for dexterous robotic grasping.

Due to the highly constrained space requirements for anthropomorphic hands, underactuated designs are widely applied. Therefore one of the most urgent research problems in humanoid hands is the efficient deployment of the available actuators to tap the highest possible amount of its potential. Overall, task-invariant synergies are thus widely applied for a variety of applications ranging from hand control to mechanical design optimization through simulation-based grasping techniques. Evidence shows that hand movements are controlled based on synergies from both biological and control point of view [1], [2].

A. Synergy Extraction

Since Santello et al. presented their first study on postural hand synergies in 1998 [2], it has been an inspiration and incentive for many researchers in robotic and prosthetic grasping. They asked subjects to imagine grasping a wide
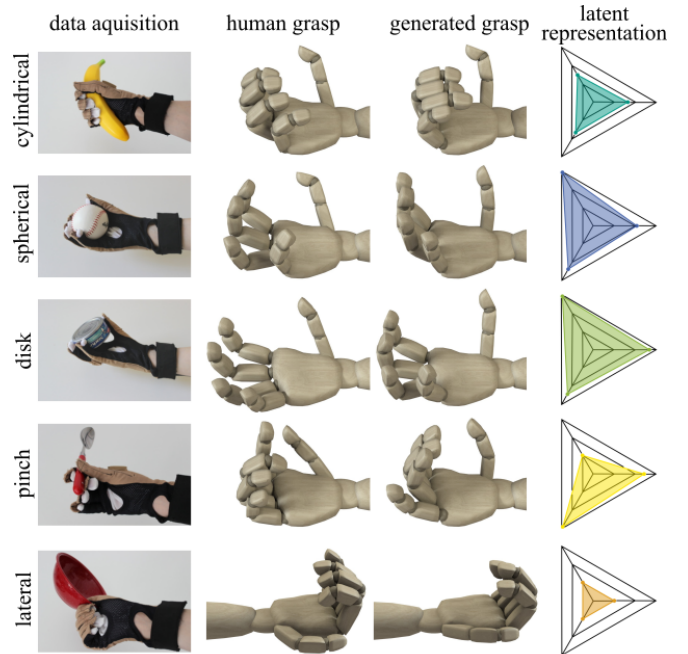
Fig. 1: The five investigated grasp types (cylindrical, spherical, disk, pinch, lateral) shown during data aquisition, from human data, generated by the presented autoencoder and the corresponding representation in the three-dimensional latent space; as two- and three-finger pinch were trained as one grasp type, the grasp generation can process a three-fingered grasp instead of a two-finger pinch for the same object width; the data is visualized on an improved version of the hand reference model of the Master Motor Map [6]

range of objects. Recorded postural hand poses were transformed with a *Principal Component Analysis* (PCA). Even the first two components accounted for more than 80% of the information generated by performing the monitored grasps. The existence of biological muscle synergies and their correlation to the postural synergies found by Santello et al. was later empirically proven in several settings [3], [4]. Soft synergies enabled the application on underactuated humanoid robotic hands [5].

Romero et al. compared PCA with several nonlinear dimensionality reduction techniques [7]. Their evaluation demonstrates, that Gaussian process latent variable models clearly outperform the results achieved by a PCA for reconstruction and generation of grasps. However nonlinear synergy-based models demand an even more complex selection of control parameters to achieve a desired grasping posture. This limits the intuitiveness of parameter selection and thus grasp control. In addition, the aforementioned study was performed with positional data describing hand and fingertip locations instead of joint angles.

B. Synergies in control

Inspired by the fundamental findings of Santello et al. [2], many following publications concentrated on the implementation of synergies in artificial hands. First approaches were entirely based on control software, mapping human synergies to an empirically or practically oriented set of robotic ones [8], [9]. To preserve a certain degree of adaptivity with respect to the actual shape of the object, the concept of soft synergies was developed [5], [10], which allows final alignment of contact surfaces despite the rigidity of the originally applied synergy-based posture. Additional enhancement covered the complete grasping process by applying temporally synchronized synergies [11]. All these approaches on synergy-based control are capable of reducing the number of control parameters. However, the achievement of specific grasping postures desired to hold or manipulate certain objects still requires an intricate selection of synergy-based values.

C. Synergies in underactuation

Mechanical synergies were first implemented for joint coupling of underactuated hands [12]. This was later extended to include serially connected shape memory alloy actuation for final grasp acquisition [13]. The model of adaptive synergies was applied in the Pisa/IIT Softhand being the most prominent example of a synergy-driven anthropomorphic hand for robotic and prosthetic purposes [14]. This concept was developed from the soft synergies exploiting the advantages of underactuation [15], [16]. Very recently the mathematical calculation of mechanically realizable manifolds of joint motions was investigated [17]. It adjusts the originally found postural synergies for their application on specific humanoid hand systems. Such underactuated designs, as applied for example in the KIT Prosthetic Hand [18], significantly decrease the control complexity allowing simpler and more robust grasp control.

Further investigation concentrated on the analytical extraction of comparable synergies for human and robotic hands. This allows the functional mapping of grasp posture [19] and the evaluation of grasp stability in synergy-based underactuated hands [20]. Also the existence of synergies in grasping force and sensing was considered and examined [21], [5]. A thorough review of synergy-based approaches to design and control of robotic hands can be found in [22].

D. Contribution

The combined impact of both object shape and grasp type on the resulting joint angles makes it difficult to directly relate grasp specific information to those low-dimensional control parameters. Selection of feasible grasps for a dedicated task is therefore challenging and little intuitive.

In this paper we present a deep autoencoder network trained with an extensive study of 2250 human grasping postures performed by 15 subjects. The network is able to generate object-specific grasps with four controlling variables. It is obliged to learn the concepts of different grasp types within a clustered three-dimensional latent space, and

object width, which is encoded in one parameter. To the best of our knowledge the developed decoder is the first method able to explicitly distinguish several grasp types and allows the generation of selected grasps on arbitrary sized objects as demonstrated in Fig. 1. The developed approach thereby aims to overcome the lack of intuition in relating existing control parameters with the required grasp contact conditions.

We consider the novel method to generate object-specific grasps and the derived understanding of the controlling synergies in human hands as the major contribution of our work. We introduce profound insights into motion coupling and inherent properties of different grasps at joint level. These findings provide interesting implications for the design and control of underactuated humanoid robotic and prosthetic hands.

II. HUMAN GRASPING STUDY

To find an intuitive set of nonlinear synergies including grasp type and object size, we trained an autoencoder with static human grasping data. To cover a wide range of human postures, 2250 grasps performed by 15 subjects holding 35 different objects with 5 grasp types were considered. The detailed information about the data acquisition is listed in Table I. In the following we describe the technical means of data acquisition and specify the structure of the sampled data.

A. Data Aquisition

The hand posture during grasp is measured with a CyberGlove III (CyberGlove Systems LLC, USA) with 18 degrees of freedom, as shown in Fig. 1. For the dimensionality reduction and resulting interpretation described in the following sections we rely on the 16 DoF which describe finger flexion and adduction as well as curvature of the palm. The remaining 2 DoF in the wrist are omitted, as they do not contribute to the grasping information for static postures.

To equalize similar hand postures independent of the actual fit of the glove, we are not evaluating the raw sensory data but use calibrated joint angles. The prior calibration of the data glove is performed with a modified version of the calibration procedure suggested by Gracia-Ibáñez et al. [23]. All finger joint angle sensors are approximated by a linear function of the sensor reading evaluating two discrete joint angles. The same procedure is applied for the palmar arch while the calibration of the combined carpometacarpal joint of the thumb is more complex. As the sensors for

TABLE I: INFORMATION ABOUT THE DATA COLLECTION

grasps	2250
subjects	15 (9 male, 6 female)
age	$27.0\,\text{years} \pm 2.0\,\text{years}$
average hand length	$180.2\,\text{mm} \pm 16.9\,\text{mm}$
minimum hand length	$144\,\text{mm}$
maximum hand length	$212\,\text{mm}$
objects	35
grasp types	5

Grasp Type	Cutkosky's Taxonomy Class [26]
cylindrical	prismatic power large diameter (1) prismatic power small diameter (2)
spherical	circular power sphere (11) circular precision sphere (13)
disk	circular power disk (10) circular precision disk (12)
pinch	prismatic precision thumb-index finger (9) prismatic precision thumb-2 finger (8)
lateral	power lateral pinch (16)

flexion and adduction are highly coupled, the calibration is widely enlarged by additional measurements. These ensure correct sensor mapping despite the complex geometry of thumb movements. In contrast to the method described by Gracia-Ibáñez et al., we apply wooden reference blocks on the palmar side of the fingers to avoid influencing the strain gauge sensors by the calibration facilities.

For all visualizations of grasp postures the distal interphalangeal joints of the long fingers, which were not measured directly, are approximated by the experimental linearization reported with the calibration procedure [23].

The achieved inter-subject variability in the joint angle measurements stays below $5°$ for all joints of the long fingers except the middle finger adduction. However the variability reveals some difficulties in thumb joint calibration especially for the metacarpophalangeal joint. This is caused by the ball of the thumb significantly impeding the formation of the correct joint angle for calibration. The mean intra-subject variability amounts to $2.94° \pm 1.32°$.

B. Performed Grasp Procedure

According to widespread studies of human grasps in common *Activities of Daily Living* (ADLs) [24], [25] we choose the five grasp types, which are present among the most frequent grasps in both works. These are a *cylindrical* wrap, a *spherical* grasp, a *disk* grasp, a *pinch* grasp and a *lateral* grasp. The subjects were asked to perform a given grasp type for each object. This eliminates manual classification of the grasp type later. We allow some flexibility for each subject to avoid an artificial bias of natural grasp performance and include a wide range of common grasping postures. Two grasps according to Cutkosky's taxonomy [26] are combined in each of our five grasp types, as can be seen in Table II. By these means we intentionally leave the final adjustment to the subject's intuition. Only the lateral grasp is directly represented by one grasp type of the applied taxonomy. Exemplary executions of the defined grasp types are additionally shown in Fig. 1.

Each of the five grasp clusters is conducted with ten objects three times each by every participant. The grasped objects are selected from the YCB Object Set [27] and the KIT Object Database [28]. A data recording session is split into the described calibration procedure and five sets. Within each set, a flat hand calibration pose is performed first. Then each of the ten objects dedicated to one grasp type is grasped three times in a row. The subjects are asked to form their grasp comparable to one of the two images of Cutkosky's taxonomy related to the current type. At the same time they should grasp in the most natural and comfortable way possible. Objects are placed directly frontal to the hand's rest position. At the end of each set, a flat hand calibration pose is adopted again.

One of the subjects was left-handed and therefore performed the grasping procedure with another instance of the sensorized glove used for data acquisition. Due to the calibration procedure, differences in performance were eliminated. A thorough examination revealed no statistically relevant differences in grasping data compared to the right-handed subjects.

A comparison of the different grasp types covered in this study shows some notable similarities especially in the spherical and disk grasp. However this similarity does not equally apply to the finger flexion behaviour. Therefore we deem it appropriate to treat spherical and disk grasps as different types.

III. DIMENSIONALITY REDUCTION

We strive to encode human grasping poses in a latent space to effectively extract and apply hand synergies. To achieve this, we propose two main requirements on the latent representation:

- **Dimensionality Reduction** The latent space should allow for low-dimensional encoding of grasp poses. This enables underactuated hand design and reduces control complexity.
- **Grasp Generation** The latent space should be encoded in a way that allows an intuitive generation of different grasp types for a given object size.

Grasps of the same type should be clustered in the latent space to allow the generation of a grasp with given type. This is hardly possible by the means of a principal component analysis, as already stated by Santello et al. They reported that differences in object shape and grasp type could only be distinguished in the higher order components carrying little overall grasping information. Therefore we employ a deep-learning based autoencoder approach, encouraged by previous studies proving that autoencoders outperform PCAs for various dimensionality reduction tasks [29], [30]. We investigated several neural network architectures. A popular approach for generation problems are variational autoencoders. Applying this approach we were able to achieve a good dimensionality reduction. However, we were not able to constrain the latent space in a way that enforces clustering of the grasp types. We therefore opted for a conventional autoencoder design. This also allowed for dimensionality reduction, however the distribution of grasps in latent space did not correlate with grasp type. Hence we added additional constraints during training of the neural network to cope with grasp type clustering.

In this section, the autoencoder architecture is described in detail and the obtained results are discussed with regard
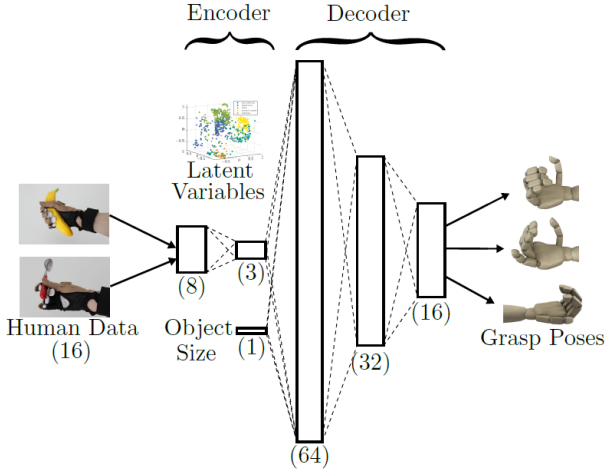
Fig. 2: Structure of the trained autoencoder; the decoder is applied as a generator for human-like grasps

Fig. 3: For training the network is provided with three samples at the same time to define the loss function

to the PCA being still the common, widely used method to compute grasp synergies.

A. Autoencoder Design

The complete architecture of the applied autoencoder is depicted in Fig. 2. The grasping joint angles are fed into the encoder. The encoder is comprised of two layers which are fully connected. For latent space we investigated different sizes starting with a dimension of two as proposed by Santello et al. for their PCA-based approach. We increased the dimensionality to three and added the object size as an additional input for the decoder. The decoder consists of three layers, which are also fully connected. As an activation function we use a hyperbolic tangent.

B. Loss Function and Training

The traditional loss function $\mathcal{L}$ for training an autoencoder-based neural network is the *Mean Squared Error* (MSE) based on the difference between input $\mathbf{y}$ and reproduced output $\widehat{\mathbf{y}}$.

$$\mathrm{MSE}(\boldsymbol{a}, \boldsymbol{b}) = \frac{1}{N} \sum_{i=1}^{N} (a_i - b_i)^2 \quad (1)$$

$$\mathcal{L} = \mathrm{MSE}\left(\boldsymbol{y}, \widehat{\boldsymbol{y}}\right) \quad (2)$$

To achieve the desired clustering, samples of the same class should be close together in the latent space, whereas samples of different classes should be separated. Therefore we consider additional terms for the loss function which are based on latent space representations. In the following we use

$$\boldsymbol{a} = \mathrm{Enc}(\boldsymbol{y}) \quad (3)$$

with $\boldsymbol{a}$ being the latent encoding and $\mathrm{Enc}(\cdot)$ representing the encoder network. A list of all used symbols can be found in Table III.

We promote aggregation of grasps $\boldsymbol{y}_g$ with the same type g in latent space by adding an additional term penalizing the mean squared distance between those grasps' latent representations $\boldsymbol{a}_g$. Separation of different grasp types $g \neq h$

is enforced by the negative incorporation of their MSE. Combining these terms we obtain the loss function

$$\begin{aligned}
\mathcal{L} = \; & \alpha \cdot \mathrm{MSE}\left(\boldsymbol{y}_g, \widehat{\boldsymbol{y}}_g\right) \\
& + \beta \cdot \mathrm{MSE}\left(\mathrm{Enc}(\boldsymbol{y}_g), \mathrm{Enc}(\boldsymbol{y}_{\widetilde{g}})\right) \\
& + \gamma \cdot \mathrm{MSE}\left(\mathrm{Enc}(\boldsymbol{y}_g), \mathrm{Enc}(\boldsymbol{y}_{h \neq g})\right) \; .
\end{aligned} \quad (4)$$

All three loss terms are weighted separately with the main emphasize put on the grasp posture reproduction as primary goal. Weighting factors are chosen as shown in Table III. The additional sample $\boldsymbol{y}_{\widetilde{g}}$ is randomly picked from the same class as $\boldsymbol{y}_g$. A schematic drawing of the loss function structure is depicted in Fig. 3. For training an Adam optimizer with a learning rate of 10^{-2} is used. To avoid overfitting and to spread out the latent space representations, we apply a normally distributed noise with a standard deviation of 0.1 on the latent space during training. This noise increases the size of the grasp type clusters and the utilization of the latent space by the encoder.

In addition to the latent variables, the decoder is provided with the object size at the grasping position. However, the size of the hand significantly influences the joint angles needed to enclose the same object. The smaller the hand, the less finger flexion is needed. Therefore the object size ranging from $1\,\mathrm{mm}$ to $140\,\mathrm{mm}$ is normalized according to the subject's hand length. This object to hand size ratio is then mapped to a span from -1 to 1 to align with the range of the original latent variables.

The data is split into training and test set with a percentage of $90\,\%$ and $10\,\%$ respectively. To ensure representable validation results, a stratified 10-fold-cross-validation is performed with all reported accuracies being the mean of the ten iterations of independent training.
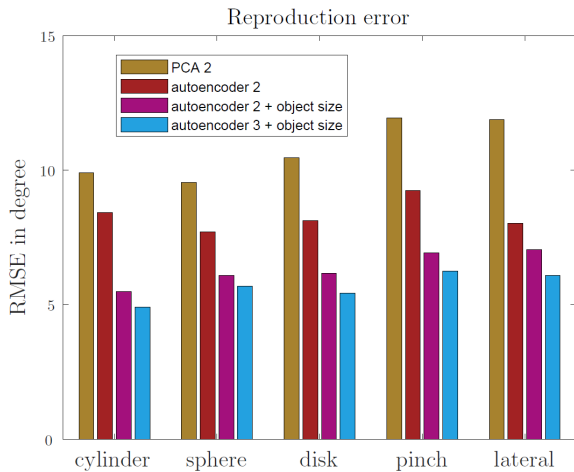
Fig. 4: Angular root mean squared error in the reproduction of human grasps for PCA and autoencoders with two variables in latent space with and without an additional parameter for object size compared to the presented autoencoder with three variables in latent space and object size

IV. EVALUATION AND INSIGHTS

The trained decoder described in the previous section possesses the ability to generate new, human-like grasps with a specified grasp type for a dedicated object size. For this purpose, the decoder has to be provided with the desired normalized object size and latent parameters. These are contained in the respective area connected with the desired grasp type in latent space. We provide a numerical evaluation of the grasps synthetically generated by the decoder. Also we come up with additional insights into human grasping behavior gained throughout the process of data acquisition and training.

A. Autoencoder Validation

Fig. 4 shows the overall reproduction error of the proposed autoencoder compared to a state-of-the-art PCA with two components and an autoencoder with only two latent variables with and without additional information on object size. It proves that an autoencoder outperforms the PCA for this dimensionality reduction by $\sim 5°$. Moreover, the introduction of object size information further reduces the overall reproduction error by $26\,\%$. The application of three latent variables compared to a two-dimensional autoencoder provides minor improvement regarding the reproduction error. However, the grasp specific distribution in latent space is more distinct for three dimensions. We therefore deem the implementation of a third latent variable appropriate to include important grasp type information into the synergy variables in a comprehensive manner. The efficiency of our efforts enforcing a partition of grasp types is visible in the ample distribution in latent space shown in Fig. 5.

The reversed autoencoder architecture applied herein yields a notably lower overall reproduction error of 5.7° compared to 7.7° with the classical mirrored design. This clearly shows that the mirrored decoder is less suited for the present case of a regression problem with enforced reinterpretation of the meanings of latent variables.
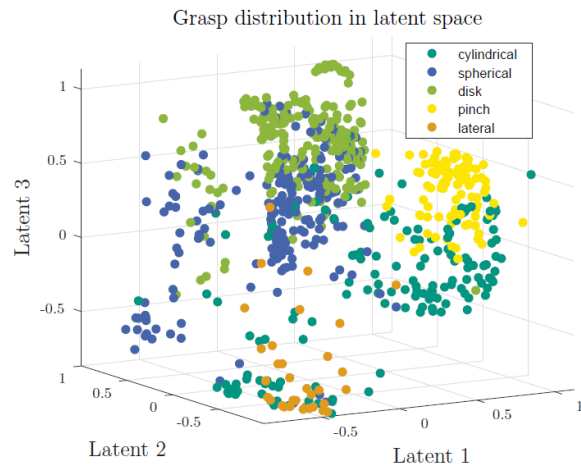
(a)
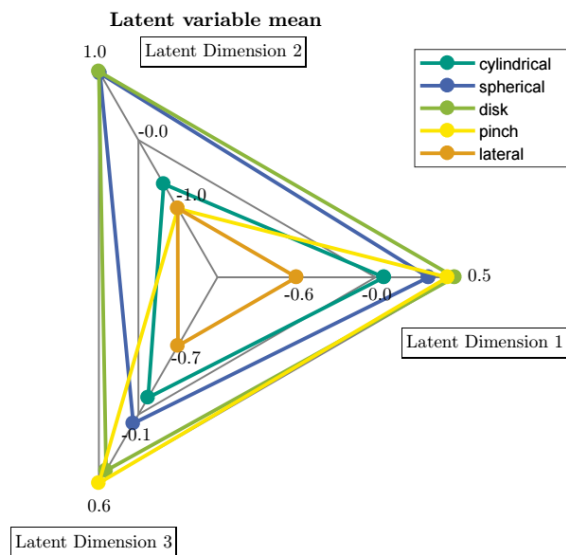
(b)

Fig. 5: Distribution of colour-coded grasp type samples in latent space (a) and the mean position of the grasp type representations (b); both visualizations show a distinct clustering of grasp types in the three-dimensional latent space allowing an intuitive generation of similar grasps by sampling the latent space near a reference grasp.

B. Quality of Generated Grasps

The generated grasps possess enough similarity with the desired human grasp type to be clearly identified as such by visual means, as shown exemplary in Fig. 1 and Fig. 6. The adaptation of object size for one grasp type is mainly notable in the metacarpophalangeal joints of the four long fingers. A clear inversely proportional correlation is identifiable by a *Pearman's Correlation Coefficient* (PCC) of -0.63 for the index joint. This pattern conforms with natural human grasping behaviour with a comparable PCC of -0.52. It proves that the association between object size and grasping joint angles is generally learned by the presented neural net as visualized in Fig. 6.

However the generated grasps also show a tendency to

$\eta = 0.01$ $\eta = 0.24$ $\eta = 0.48$

$\eta = 0.72$ $\eta = 0.88$ $\eta = 0.97$
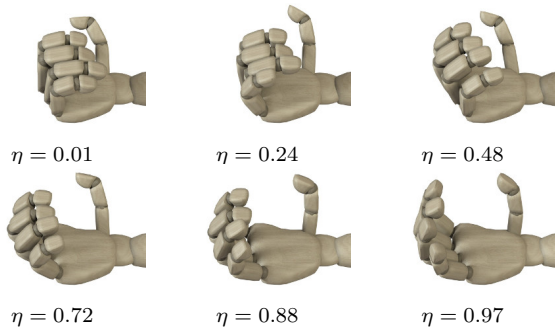
Fig. 6: Series of generated cylindrical grasps with the ratio η of object size to hand length

correlate finger adduction and grasp size which is not present in human cylindrical grasps. The reason for this discrepancy lies in the direct neighbourhood of cylindrical and disk grasps in latent space. It causes the decoder to transfer some of the finger adduction applied in disk grasps to the object size information. An additional challenge in grasp size reproduction is the variability in hand sizes for the human subjects. The necessary amount of finger flexion needed to enclose an object is dependent of the object size and the length ratio of the finger phalanges. As the decoder is trained with grasping data for a wide range of hand sizes, this causes a notable variance in actual grasp width of generated grasps. To overcome these challenges in grasp stability the generated grasps are handled as soft synergies, thereby providing additional flexibility also to non-static object size.

C. Latent Distribution

Similar to the principal components obtained by a linear analysis, the latent variables of the trained autoencoder reveal valuable insights into positional couplings of human grasp postures. However, the influence of each individual variable on the overall position is less apparent due to the nonlinear coding, which in turn allows the stringent partition of grasp types in the first place. The three latent variables will be further denoted as l_1, l_2 and l_3 for brevity. Considering the distribution of the mean latent description of each grasp type depicted in Fig. 5, the two pairs of spherical and disk grasp and pinch and lateral grasp clearly share the same activation respectively in l_2. A third similarity becomes apparent between disk and pinch grasp in l_1.

The synergy described by l_1 is the only one controlling the thumb interphalangeal joint in its full range of motion and thereby allowing an entire extension of the thumb. This is mainly required in pinch grasps, where the thumb is needed as rigid support the object is pressed against by the fingers. But also in disk grasps the thumb itself is left nearly straight as proven by the similar activation of l_1. For a lateral grasp on the contrary a high thumb flexion is fundamental. The metacarpophalangeal joints of index, middle and ring finger are also mainly - but not only - controlled by l_1.

l_2 primarily controls the finger adduction joints, causing the mentioned segmentation in open, adducted grasps as spherical and disk in opposition to compact, abducted grasps like pinch and lateral.

Fine tuning of proximal interphalangeal joints is mainly performed by the third synergy. Within this parameter, cylindrical and spherical grasp are more closely resemblant than compared to the disk grasp, as the former types both enclose a round surface with the fingers. The disk grasp on the contrary directs them along the longitudinal axis of the object. A notable tendency to completely close all long fingers when grasping laterally is reflected in l_3.

D. Control Implications

Reviewing the joint angle regulation by the three latent variables and the behaviour of different grasp types for varying object width some general observations for static grasping postures can be derived. The tendency in the latent variables to mainly control one type of joints can be proven in human grasping data especially for cylindrical, spherical and disk grasps. Mean of PCC in metacarpophalangeal joints are 0.69, 0.68 and 0.49 for the index compared to the other three long fingers in human data. The same applies to the correlation in proximal interphalangeal joints with 0.68, 0.55 and 0.42 and adduction joints with 0.59 for middle finger compared to both ring and little finger. Generally it can be noted, that correlation becomes weaker to the ulnar side of the hand. In comparison to the thumb as opposing part, the positioning of the index and middle finger is more strictly defined than the ring and index, although the latter two tend to follow as much as object shape and grasp intention allow.

There is also an interesting correlation between the thumb carpometacarpal joint and palmar arch, mainly notable in cylindrical grasps with PCC of 0.69. Additional observations reveal a gentle physical coupling between both joints, causing the whole palm to curve when the thumb is opposed to the fingers. However, the angular measurement of this motion by a strain gauge along the dorsal side of the knuckles can be superimposed by a hyperextension of the little finger. Therefore it is less prominent in the other grasp types.

V. CONCLUSION

This paper presents a study of human grasping postures including 2250 grasps performed by 15 subjects on 35 different objects. The gathered data is analyzed by means of a deep-learning based autoencoder approach. We demonstrated that we are able to represent the grasps in a low-dimensional latent space. Different neural network architectures were evaluated regarding their performance for the dimensionality reduction of joint angle data and the intelligibility of grasp properties within the latent variables. The chosen autoencoder with three-dimensional latent space outperforms the state-of-the-art PCA by a decrease of 47% for the reproduction error.

The resulting latent space allows for several key observations: Grasps of the same type are clustered together. The clusters of dissimilar types are spaced far apart in latent space. This is most prominent for the lateral grasp type. The grasp clusters of related grasp types are placed close to each

other with a fluent transition. This can be seen for spherical and disk grasps, as can be expected, since both types fall within the circular grasps according to Cutkosky [26].

Due to the intuitive layout of the latent space we are able to generate object-specific grasps. For generation we can specify the desired grasp type by choosing a latent sample within one of the grasp clusters. Furthermore we can generate the grasp for different object sizes by setting the independent object size parameter of the decoder network.

The comprehensible grasp representation offers further insights into joint couplings and grasp specific features in human hand postures presented by this work. For example the coupling of finger adduction and hand aperture is captured by the decoder. We believe that these insights are of great assistance for further development of control algorithms allowing an intuitive parameter selection. They also facilitate the decision on sensible hardware simplifications by underactuated coupling in robotic and prosthetic hands.

In future work we are planning to further analyze the found synergies in the latent space and investigate the applicability of generative adversarial networks for the problem at hand. Nonetheless we see the insights on synergy-related human joint positions gained herein as a fascinating incentive for future development of synergy-driven anthropomorphic hands. Especially for prosthetics and lightweight humanoid robot hands, where compact but versatile systems are required, these findings will contribute to the design of advanced actuating mechanisms.

REFERENCES

[1] J. N. Ingram, K. P. Körding, I. S. Howard, and D. M. Wolpert, "The statistics of natural hand movements," *Experimental Brain Research*, vol. 188, no. 2, pp. 223–236, 2008.

[2] M. Santello, M. Flanders, and J. F. Soechting, "Postural Hand Synergies for Tool Use," *The Journal of Neuroscience*, vol. 18, no. 23, pp. 10 105–10 115, 1998.

[3] E. J. Weiss and M. Flanders, "Muscular and Postural Synergies of the Human Hand," *Journal of Neurophysiology*, vol. 92, no. 1, pp. 523–535, 2004.

[4] C. Castellini and P. Van Der Smagt, "Evidence of muscle synergies during human grasping," *Biological Cybernetics*, vol. 107, no. 2, pp. 233–245, 2013.

[5] A. Bicchi, M. Gabiccini, and M. Santello, "Modelling natural and artificial hands with synergies," *Philosophical Transactions of the Royal Society B: Biological Sciences*, vol. 366, no. 1581, pp. 3153–3161, 2011.

[6] C. Mandery, O. Terlemez, M. Do, N. Vahrenkamp, and T. Asfour, "Unifying representations and large-scale whole-body motion databases for studying human motion," *IEEE Transactions on Robotics*, vol. 32, no. 4, pp. 796–809, August 2016.

[7] J. Romero, T. Feix, C. H. Ek, H. Kjellström, and D. Kragic, "Extracting Postural Synergies for Robotic Grasping," *IEEE Transactions on Robotics*, vol. 29, no. 6, pp. 1342–1352, 2013.

[8] M. T. Ciocarlie and P. K. Allen, "Hand Posture Subspaces for Dexterous Robotic Grasping," *Int. Journal of Robotics Research*, vol. 28, no. 7, pp. 851–867, 2009.

[9] T. Wimböck, J. Reinecke, and M. Chalon, "Derivation and Verification of Synergy Coordinates for the DLR Hand Arm System," in *IEEE Int. Conf. on Automation Science and Engineering*, 2012, pp. 454–460.

[10] M. Gabiccini, A. Bicchi, D. Prattichizzo, and M. Malvezzi, "On the Role of Hand Synergies in the Optimal Choice of Grasping Forces," *Autonomous Robots*, vol. 31, no. 2-3, pp. 235–252, 2011.

[11] B. A. Kent, J. Lavery, and E. D. Engeberg, "Anthropomorphic Control of a Dexterous Artificial Hand via Task Dependent Temporally Synchronized Synergies," *Journal of Bionic Engineering*, vol. 11, no. 2, pp. 236–248, 2014.

[12] C. Brown and H. Asada, "Inter-Finger Coordination and Postural Synergies in Robot Hands Via Mechanical Implementation of Principal Components Analysis," in *IEEE/RSJ Int. Conf. on Intelligent Robots and Systems*, 2007, pp. 2877–2882.

[13] J. B. Rosmarin and H. H. Asada, "Synergistic Design of a Humanoid Hand with Hybrid DC motor-SMA Array Actuators Embedded in the Palm," in *IEEE Int. Conf. on Robotics and Automation*, 2008, pp. 773–778.

[14] S. B. Godfrey, A. Ajoudani, M. Catalano, G. Grioli, and A. Bicchi, "A synergy-driven approach to a myoelectric hand," in *IEEE Int. Conf. on Rehabilitation Robotics*, 2013.

[15] M. G. Catalano, G. Grioli, A. Serio, E. Farnioli, C. Piazza, and A. Bicchi, "Adaptive Synergies for a Humanoid Robot Hand," in *IEEE-RAS Int. Conf. on Humanoid Robots*, 2012, pp. 7–14.

[16] M. Catalano, G. Grioli, E. Farnioli, A. Serio, C. Piazza, and A. Bicchi, "Adaptive Synergies for the Design and Control of the Pisa/IIT SoftHand," *Int. Journal of Robotics Research*, vol. 33, no. 5, pp. 768–782, 2014.

[17] T. Chen, M. Haas-Heger, and M. Ciocarlie, "Underactuated Hand Design Using Mechanically Realizable Manifolds," in *IEEE Int. Conf. on Robotics and Automation*, 2018, pp. 7392–7398.

[18] P. Weiner, J. Starke, F. Hundhausen, J. Beil, and T. Asfour, "The KIT Prosthetic Hand: Design and Control," in *IEEE/RSJ Int. Conf. on Intelligent Robots and Systems*, 2018, to be published.

[19] D. Prattichizzo, M. Malvezzi, M. Gabiccini, and A. Bicchi, "On Motion and Force Controllability of Precision Grasps with Hands Actuated by Soft Synergies," *IEEE Transactions on Robotics*, 2013.

[20] M. Gabiccini, E. Farnioli, and A. Bicchi, "Grasp and Manipulation Analysis for Synergistic Underactuated Hands Under General Loading Conditions," in *IEEE Int. Conf. on Robotics and Automation*, 2012, pp. 2836–2842.

[21] M. Santello and J. F. Soechting, "Force synergies for multifingered grasping," *Experimental Brain Research*, vol. 133, no. 4, pp. 457–467, 2000.

[22] M. Santello, M. Bianchi, M. Gabiccini, E. Ricciardi, G. Salvietti, D. Prattichizzo, M. Ernst, A. Moscatelli, H. Jörntell, A. M. Kappers, K. Kyriakopoulos, A. Albu-Schäffer, C. Castellini, and A. Bicchi, "Hand synergies: Integration of robotics and neuroscience for understanding the control of biological and artificial hands," *Physics of Life Reviews*, vol. 17, pp. 1–23, 2016.

[23] V. Gracia-Ibáñez, M. Vergara, J. H. Buffi, W. M. Murray, and J. L. Sancho-Bru, "Across-subject calibration of an instrumented glove to measure hand movement for clinical purposes," *Computer Methods in Biomechanics and Biomedical Engineering*, vol. 19, no. August, pp. 1–11, 2017.

[24] I. Bullock, J. Z. Zheng, S. De La Rosa, C. Guertler, and A. M. Dollar, "Grasp Frequency and Usage in Daily Household and Machine Shop Tasks," *IEEE Transactions on Haptics*, vol. 6, no. 3, pp. 296–308, 2013.

[25] M. Vergara, J. L. Sancho-Bru, V. Gracia-Ibáñez, and A. Pérez-González, "An introductory study of common grasps used by adults during performance of activities of daily living," *Journal of Hand Therapy*, vol. 27, no. 3, pp. 225–234, 2014.

[26] M. R. Cutkosky, "On Grasp Choice, Grasp Models, and the Design of Hands for Manufacturing Tasks," *IEEE Transactions on Robotics and Automation*, vol. 5, no. 3, pp. 269–279, 1989.

[27] B. Calli, A. Walsman, A. Singh, S. Srinivasa, P. Abbeel, and A. Dollar, "Benchmarking in Manipulation Research : The YCB Object and Model Set and Benchmarking Protocols," *IEEE Robotics & Automation Magazine*, vol. 22, no. 3, pp. 184–185, 2015.

[28] A. Kasper, Z. Xue, and R. Dillmann, "The KIT object models database: An object model database for object recognition, localization and manipulation in service robotics," *Int. Journal of Robotics Research*, vol. 31, no. 8, pp. 927–934, 2012.

[29] Y. Wang, H. Yao, and S. Zhao, "Auto-encoder based dimensionality reduction," *Neurocomputing*, vol. 184, pp. 232–242, 2016.

[30] P. Baldi and K. Hornik, "Neural Networks and Principal Component Analysis: Learning from Examples Without Local Minima," *Neural Networks*, vol. 2, no. 10, pp. 53–58, 1989.